Critical Properties of Three Dimethyl Ether Binary Systems: Dimethyl Ether (RE-170) + Propane (HC-290), Butane (HC-600), and 2-Methyl Propane (HC-600A)

Masahiko Yasumoto,[†] Yuko Uchida,[‡] Kenji Ochi,[‡] Takeshi Furuya,[†] and Katsuto Otake*,[†]

Nanotechnology Research Institute, National Institute of Advanced Industrial Science and Technology, Tsukuba Central 5, Higashi 1-1-1, Tsukuba, Ibaraki 305-8565, Japan, and College of Science & Technology, Nihon University, Kanda-Surugadai 1-8-14, Chiyoda-ku, Tokyo 101-8308, Japan

Critical properties of dimethyl ether (DME, RE-170) and its three binary mixtures with hydrocarbons, propane (HC-290), butane (HC-600), and 2-methyl propane (HC-600a), were measured with uncertainties of ±10 mK in temperature, ±0.5 kPa in pressure, ±1 kg m^{-3} in density, and ±0.5% in composition. The experimental data were correlated by equations proposed by Higashi.

1. Introduction

Dimethyl ether (DME) is currently under discussion as a possible additive to diesel fuel on account of its ability to reduce particle emission.[1] Further, it is well-established as a propellant in the aerosol industry,[2,3] as an alternative working fluid for absorption heat pumps,[4] in supercritical extraction systems,[5] and also as an alternative fuel for portable polymer electrolyte fuel cells.[6] Due to regulations on the use of volatile organic compounds (VOCs) and the emission of particulates in diesel exhaust, the industrial exploitation of DME seems highly promising.

For the safe introduction of DME, however, a broad understanding of the major physicochemical properties of the compound is clearly very important. Critical constants (critical temperature, critical pressure, and critical density) are among the most important values used for the estimation and calculation of physicochemical properties.

In previous papers, we reported on the construction of an apparatus for the precise measurement of critical parameters using only small sample amounts,[7] and we measured those of pure[7,8] and mixed substances.[9,10] In the current work, the critical constants and vapor pressure of DME were measured. In addition, the critical loci of the mixtures of DME and some low molecular weight hydrocarbons (propane, butane, and 2-methyl propane) important for questions of DME utilization in fuels were also measured.

2. Experimental Section

Materials. Table 1 summarizes the molecular formulas and molar based purities for all compounds used in this study. The DME was supplied by Sumitomo Seika Chemicals Co., Ltd. All other hydrocarbons were purchased from Takachiho Chemical Industrial Co., Ltd.

Purities were analyzed by gas chromatography (Hewlett-Packard, model HP-6890, thermal conductivity detector).

Table 1. Properties of Samples

name	molecular formula	purity/mol %
dimethyl ether (DME)	CH_3OCH_3	99.9
propane	$CH_3CH_2CH_3$	99.9
butane	$CH_3CH_2CH_2CH_3$	99.9
2-methyl propane	$(CH_3)_2CHCH_3$	99.9

Apparatus. The critical parameters of the mixtures were measured by observing the behavior of the meniscus at the vapor−liquid interface in an optical cell. The experimental apparatus (Figure 1) used in this study was the same as that described earlier.[7−10] The optical cell was connected to the two variable volume vessels and the differential null-pressure detector by a valve (V_1). The central axis of these vessels and the detector were adjusted to be at the same level. The temperature of the oil bath was controlled to within 3 mK in the range (300 to 450) K. Under these conditions, the uncertainty in the critical temperature is estimated to be ±10 mK. The uncertainties in pressure, density, and composition were estimated to be less than ±0.5 kPa, ±1 kg m^{-3}, and ±0.5% (molar base), respectively. The apparatus was specially designed for critical parameter measurements with small sample sizes and needs only (5 to 6) mL for a single experiment.

Procedure: Sample Preparation. Procedures for the preparation of sample mixtures and the measurement of critical properties are described in previous papers.[9,10] Mixtures of composition selected for investigation were prepared with the apparatus shown in Figure 2. From stainless steel sample cylinder A, sample 1 was transferred to glass cylinder D to roughly measure the amount of sample and then to stainless steel cylinder C using hot water and liquid nitrogen. Cylinder C was disconnected from the vacuum line, weighed, and reconnected. Then, from stainless steel cylinder B, sample 2 was transferred to cylinder D and then to cylinder C to mix with sample 1. Cylinder C was disconnected and weighed. The initial composition of the sample mixture was calculated from the mass ratio of pure samples in cylinder C. Cylinder C was reconnected again, and the sample mixture was transferred to glass cylinder E and loaded into the optical cell situated in a constant temperature air bath at 253 K under vacuum. After (80 to 90)% of the optical cell was filled with the liquid

---

* Corresponding author. Phone: +81-298-61-4567 or +81-298-61-4819. Fax: +81-298-61-4567. E-mail: katsuto-otake@aist.go.jp.
[†] National Institute of Advanced Industrial Science and Technology.
[‡] Nihon University.

10.1021/je0496589 CCC: $30.25

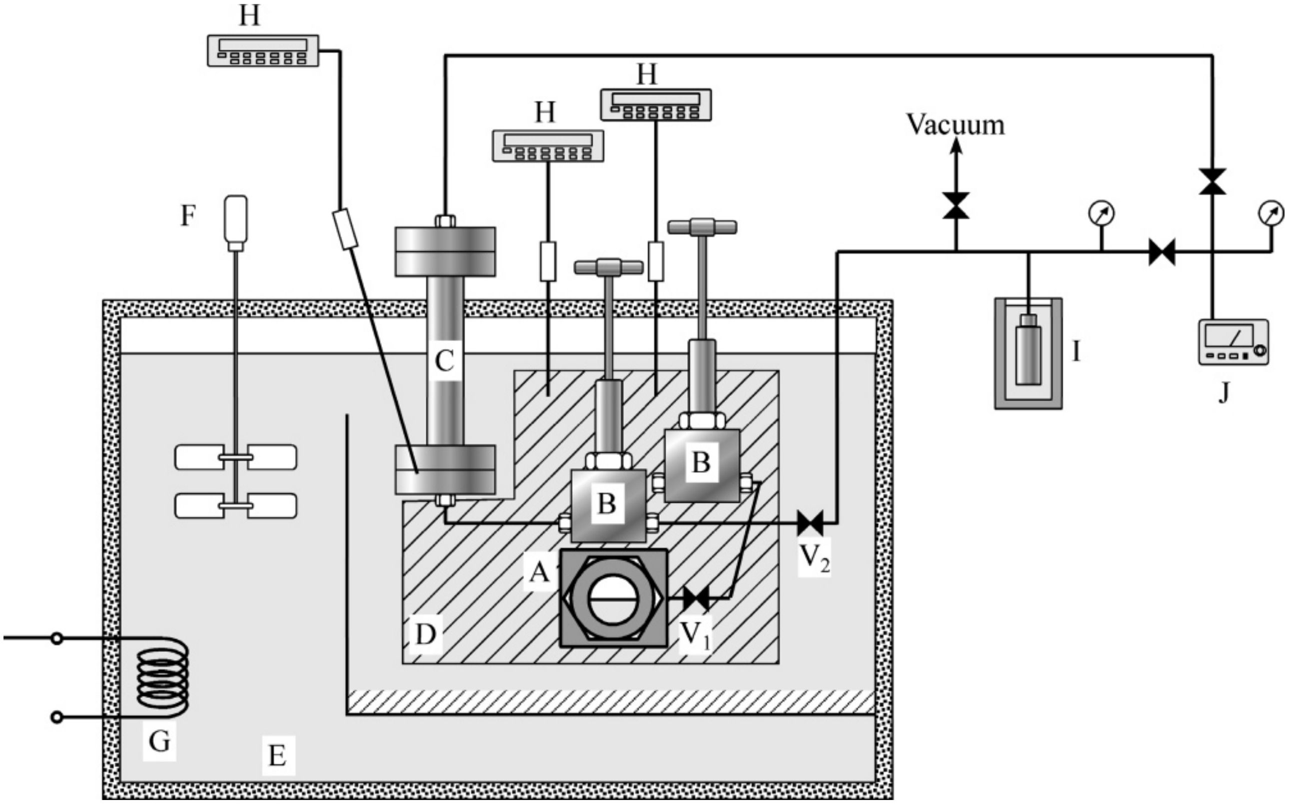

Figure 1. Experimental apparatus: A, optical cell; B, variable volume vessel; C, differential null-pressure detector; D, aluminum blocks; E, constant temperature oil bath; F, stirrer; G, temperature controller; H, platinum resistance thermometer; I, cold trap; J, quartz crystal pressure gauge; V$_1$, cutoff valve; V$_2$, separation valve.

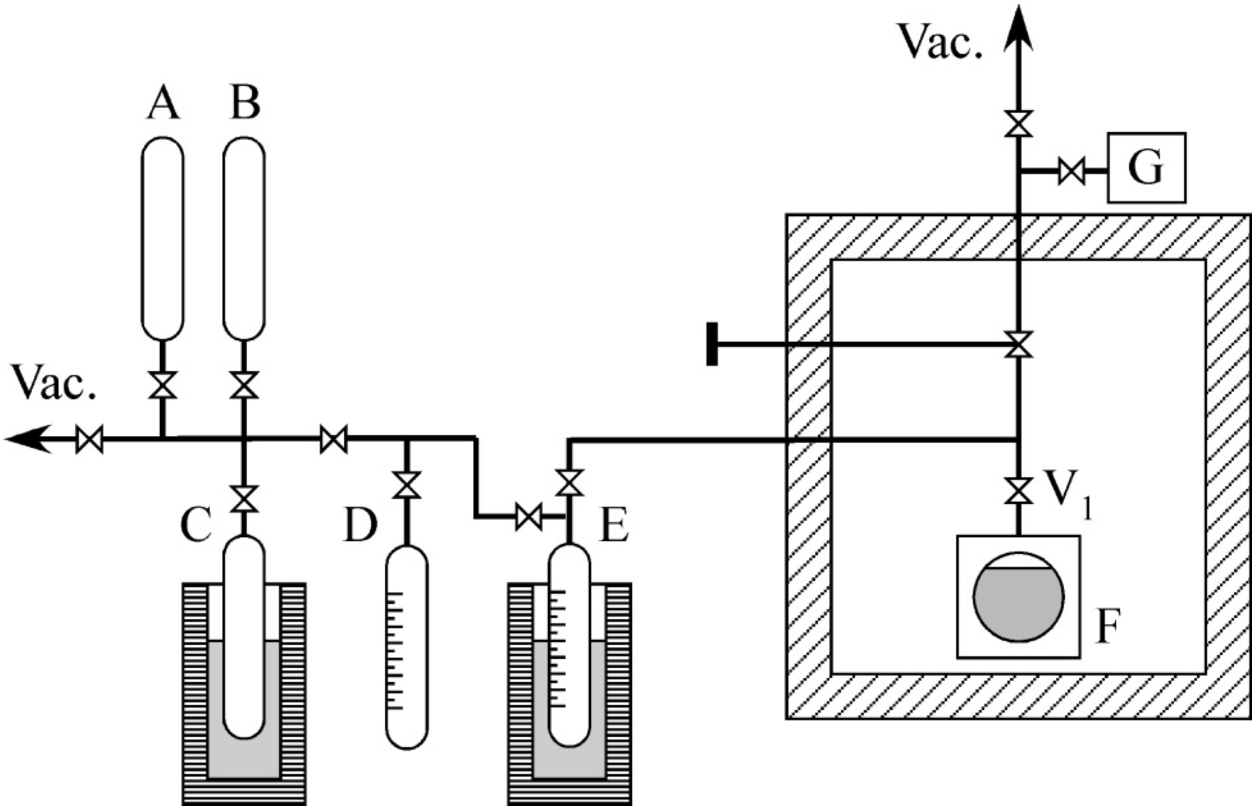

Figure 2. Apparatus for sample loading: A and B, stainless steel cylinder for storing components A and B; C, stainless steel cylinder for purification; D and E, glass cylinder for purification and volume measurement; F, optical cell; G, pressure gauge.

mixture, the cell was disconnected from the apparatus at valve V$_1$ and connected to the critical parameter measurement apparatus shown in Figure 1.

Procedure: Critical Parameter Measurements. After the optical cell was connected to the main apparatus (Figure 1, at V$_1$), the remaining part of the apparatus was

Table 2. Comparison of the Critical Parameters

	author	T_C/K	P_C/MPa	ρ_C/kg m^{-3}	note
dimethyl ether (CH_3OCH_3) (RE-170)	Nadezhdin et al.[14]	402.8			a
	Ledue et al.[14]		5.8		a
	Briner et al.[14]	400	5.4		a
	Briner et al.[14]	400.2	5.4		a
	Cardoso et al.[14]	400.0	5.27		a
	Cardoso et al.[14]			271.4	a
	Winkler et al.[14]	399.4	5.4		a
	Winkler et al.[14]	399.6			a
	Tapp et al.[14]	400.0		225.5	a
	Edwards et al.[14]	400.0	5.33	246.5	a
	Pall et al.[14]	400.0			a
	Oshipiuk et al.[14]	400			a
	Zawisza et al.[14]	400.3	5.359	281	a
	Noles et al.[21,24]	399.40	5.270		a
	Noles et al.[25,26]	399.4	5.264		a
	Kudchadker et al.[14]	400.2	5.34	275	b
	Wu et al.[27]	400.378	5.3558		a
	Wu et al.[28]	400.378	5.356	272	a
	Tsuji[29]	399.60	5.293	288.6	b
	this work	399.63	5.268	271	a
propane (HC-290)	Stryjek et al.[30]	369.82	4.24953		a
	Younglove et al.[12]	369.83	4.24766	220.5	a
	Brunner et al.[12]	369.89	4.260		a
	Sychev et al.[12]	369.83	4.2475	220.49	a
	Ambrose et al.[12]	369.83	4.248	220	b
	Higashi[31]	369.818	4.2465	227	a
	Higashi[17]	369.818	4.2465	227	a
	this work	369.84	4.247	216	a
butane (HC-600)	Stryjek et al.[30]	425.16	3.79661		a
	Younglove et al.[12]	425.12	3.796	227.8	a
	Brunner et al.[12]	425.06	3.793		a
	Li et al.[12]	424.6	3.80	221	a
	Ambrose et al.[12]	425.12	3.796	228	b
	this work	425.16	3.787	225	a
2-methyl propane (HC-600a)	Goodwin et al.[13]	407.82	3.640	224	a
	Sengers et al.[32]	407.84	3.629	225.5	a
	Waxman et al.[13]	407.82	3.629	227	a
	Levelt et al.[13]	407.81	3.629	225.5	a
	Younglove et al.[13]	407.82	3.640	224.4	a
	Daubert[13]	407.8	3.640	224	b
	Higashi[31]	407.795	3.6282	229	a
	this work	407.81	3.633	225	a

[a] Experimental data. [b] Estimated or recommended data.

Table 3. Vapor Pressure of DME

temperature/K	pressure/MPa	temperature/K	pressure/MPa
303.14	0.6790	363.31	2.7330
306.71	0.7496	373.34	3.3062
313.09	0.8883	373.34	3.3060
313.09	0.8877	383.37	3.9678
323.14	1.1433	383.38	3.9678
323.15	1.1432	393.41	4.7309
333.18	1.4491	393.41	4.7315
333.18	1.4494	399.62	5.2670
343.22	1.8116	399.63[a]	5.2680[a]
343.23	1.8126		
353.25	2.2369		
353.28	2.2377		
363.30	2.7323		

[a] Critical temperature and pressure.

Table 4. Wagner Constants

Wagner constants (AAD = 0.014%)
$a = -6.983$
$b = 1.541$
$c = -1.677$
$d = -3.294$

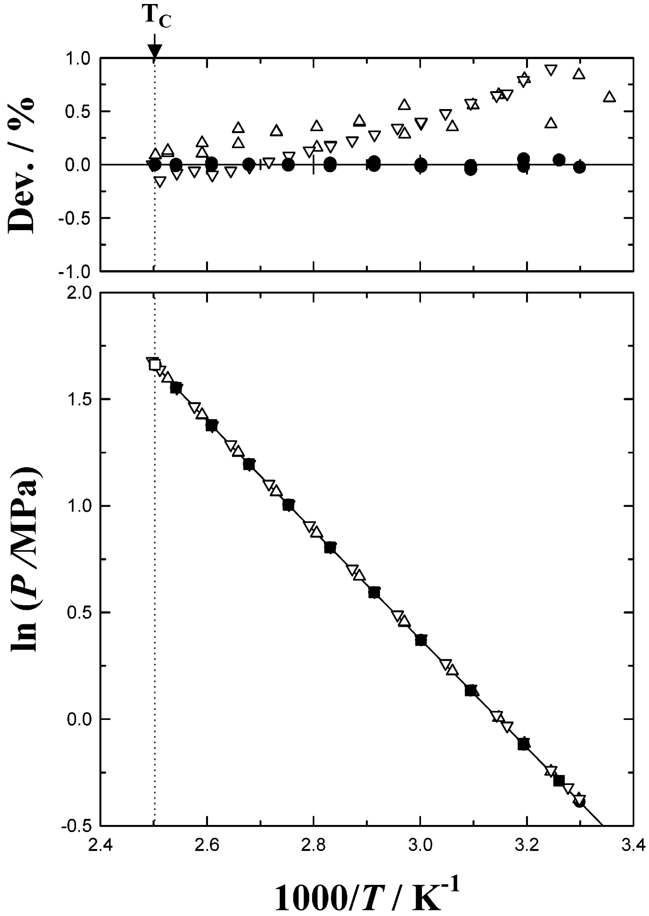

Figure 3. Vapor pressure of DME correlated by the Wagner equation: ●, this work (vapor pressure, run 1); ■, this work (vapor pressure, run 2); ○, this work (critical constant, run 1); □, this work (critical constant, run 2); △, Florusse et al.; ▽, Wu et al. Deviation/% = [(exptl − calcd)/exptl] × 100.

evacuated. Valve V_2 was closed, and the temperature was raised to ~10 K higher than the room temperature. After temperature fluctuations became < ±5 mK, V_1 was opened to fill the apparatus. As the inner volume of the apparatus including the optical cell, null-pressure detector, and piping was ~10 cm^3 and that of the optical cell was ~5 cm^3, the meniscus of the optical cell positions about the center of the viewing windows after the sample addition.

After the pressure fluctuations became < ±0.1 kPa, they were recorded, and V_1 was closed and the temperature was raised in 10 K increments to near the critical temperature. In every temperature step described above and in the following paragraphs, at least 1 h of equilibration was allowed to stabilize the temperature fluctuations till they became < ±5 mK before opening V_1 to measure the pressure and the difference in pressures with V_1 opened and closed. As can be seen from Figure 1, the null-pressure detector and the observation cell were connected by $^1/_8$ in. tubing. If a composition difference does exist, the difference in pressure with and without V_1 open becomes significant. For the precise determination of the critical parameters, uniformity of composition must be achieved. If V_1 was kept open during the change in temperature, an identical composition of sample between the optical cell and null-pressure detector could not be achieved even with more than 24 h of composition equilibration in the supercritical state condition shown below. At the same time, after opening V_1, equilibration time was allowed until the pressure fluctuations became < ±0.1 kPa before recording the pressure.

When the temperature was 10 K lower than the critical temperature estimated by Joback's method,[11] the temperature steps were decreased to (1 to 5) K. The position of the meniscus was adjusted after opening V_1 by the variable volume vessels at the center of the viewing window. When

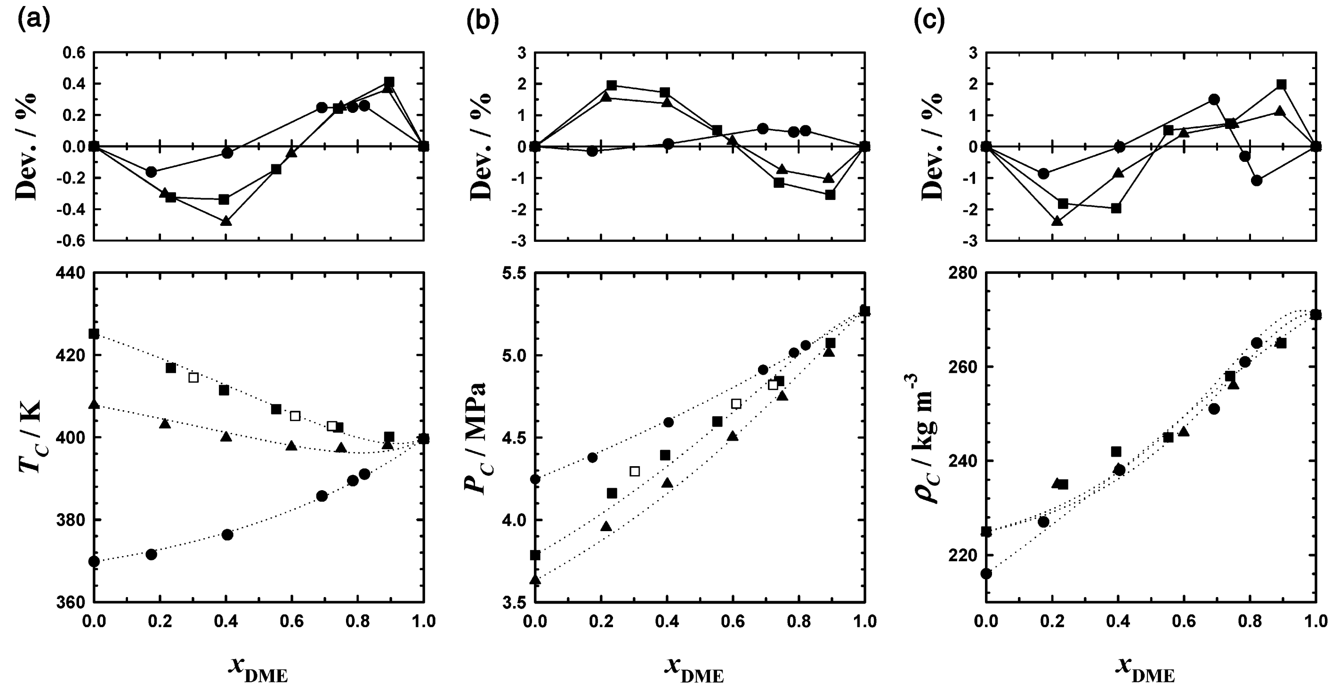

Figure 4. Critical parameters of the binary mixtures of DME and hydrocarbons; (a) critical temperature, (b) critical pressure, and (c) critical density: ●, propane; ■, butane; ▲, 2-methyl propane; □, butane (Defernandez et al.). The dotted lines are the correlated results by eqs 4−9. Deviation/% = [(exptl − calcd)/exptl] × 100.

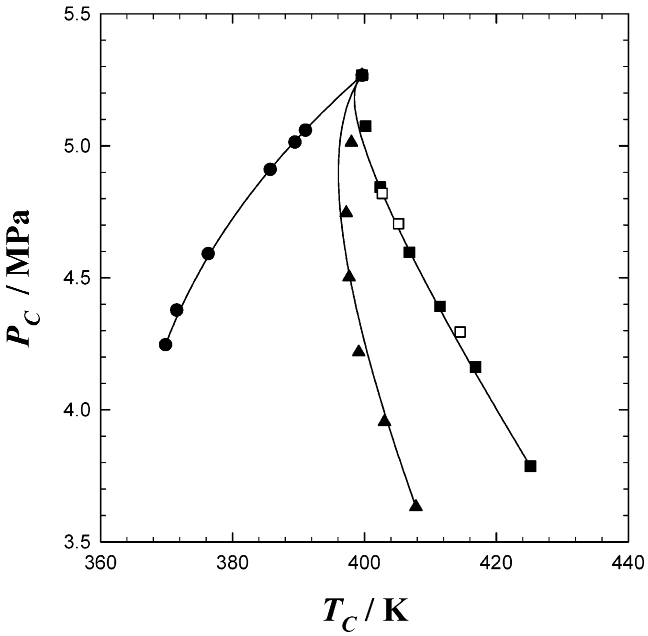

Figure 5. Critical loci of the binary mixtures of DME and hydrocarbons: ●, propane; ■, butane; ▲, 2-methyl propane; □, butane (Defernandez et al.). The lines are the correlated results by eqs 4−9.

the temperature exceeded the critical temperature, which was confirmed by the disappearance of the meniscus, the temperature was decreased in 100 mK steps until the reappearance of the meniscus occurred.

After the reappearance of the meniscus, the temperature was increased again in 10 mK increments, with observation of the critical opalescence. After reaching the supercritical state again, after the equilibration, V_1 was opened, and the inner volume of the system was controlled by the variable volume vessels following the appearance of the critical opalescence during the temperature increase: if the critical opalescence appeared more intent in the vapor phase than in the liquid phase, which means the density in the system is higher than the critical density,[9,10] the inner volume was increased. On the other hand, if the critical opalescence appeared more intent in the liquid phase, which means the density is lower than the critical density,[9,10] the inner volume was decreased. Then, V_1 was closed, and the temperature was decreased in 10 mK steps until the meniscus reappeared. These procedures for the adjustment of the position of the meniscus were repeated several times to give an equally strong critical opalescence in both the vapor and liquid phases.

After adjusting the position of the meniscus, the temperature was decreased again in 10 mK increments, with observation of the critical opalescence. The temperature at which the inside of the optical cell becomes black, T_{CL}, was determined, and the temperature was set to T_{CL} − 10 mK. Then, the temperature was increased in 10 mK increments, with observation of the meniscus. The temperature at which the critical opalescence becomes most intent and the meniscus becomes thick, T_{CH}, was determined, and the temperature was set to T_{CH} + 10 mK. In general, T_{CH} is always (10 to 20) mK higher than T_{CL}. These procedures were repeated several times, and the critical temperature was determined as $T_C = (T_{CL} + T_{CH})/2$. The critical pressure was determined from the linear interpolation of the pressures measured in the temperature steps around the critical temperature.

It should be noted that the change in inner volume of the apparatus by the variable volume vessels was conducted always in the supercritical state. The procedures described above were developed especially to ensure uniform composition of samples in the apparatus.

After the critical parameter measurements, the samples inside the optical cell and the null-pressure detector were trapped in the cold trap (Figure 1, I) separately and weighed. The critical density was then determined from the mass of the sample in the trap and the known internal volume of the optical cell. The compositions of the samples were analyzed by the gas chromatograph.

Table 5. Critical Parameters of the DME (1) + Propane (2) System

x_1[a]	T_C/K	P_C/MPa	ρ_C/kg m^{-3}	x_1[b] (optical cell base deviation/%)[c]	x_1[d] (optical cell base deviation/%)[e]
0.0000	369.84	4.247	216	0.0000 (0.00)	0.0000 (0.00)
0.1741	371.54	4.377	227	0.1763 (−1.26)	0.1752 (−0.63)
0.4049	376.31	4.591	238	0.4079 (−0.74)	0.4056 (−0.17)
0.6913	385.72	4.910	251	0.7025 (−1.62)	0.6889 (0.35)
0.7849	389.45	5.014	261	0.7838 (0.14)	0.7864 (−0.19)
0.8205	391.05	5.059	265	0.8199 (0.07)	0.8211 (−0.07)
1.0000	399.63	5.267	271	1.0000 (0.00)	1.0000 (0.00)
			AAD:	**(0.55)**	**(0.20)**

[a] Mole fraction in the optical cell. [b] Mole fraction calculated from the weight ratio. [c] $100(x_{\text{optical cell}} - x_{\text{feed}})/x_{\text{optical cell}}$. [d] Mole fraction in the null-pressure detector and variable volume vessels. [e] $100(x_{\text{optical cell}} - x_{\text{null-pressure detector}})/x_{\text{optical cell}}$.

3. Results and Discussion

Critical Parameters of Pure Substances and Vapor Pressure of DME. The critical parameters of the pure substances used in this study are summarized in Table 2 together with literature data. From the table, the critical parameters of hydrocarbons are seen to be almost identical to the literature values as well as recommended values.[12,13] On the other hand, the critical parameters, especially the critical temperature, of DME are somewhat different. As could be seen from the table, most reported critical values for DME lie between (399.4 and 400.3) K, (5.24 and 5.8) MPa, and (225.5 and 288.6) kg m^{-3} for T_C, P_C, and ρ_C, respectively. The recommended critical parameters of DME are 400.2 ± 0.1 K, 5.34 ± 0.05 MPa, and 275 ± 10 kg m^{-3}, respectively.[14] Our current results (399.63 K, 5.268 MPa, and 271 kg m^{-3}) fall in these ranges. Further, the critical parameters for the hydrocarbons coincided well with the literature data. From these facts, our current critical parameters of DME would be acceptable and reliable.

The saturated vapor pressures of DME are tabulated in Table 3 and shown in Figure 3 together with the data of Florusse et al.[5] and Wu et al[22] and with correlated results using the Wagner equation:[11]

$$\ln P_r = \frac{a(1 - T_r) + b(1 - T_r)^{1.5} + c(1 - T_r)^{2.5} + d(1 - T_r)^5}{T_r} \tag{1}$$

$$P_r = P/P_C \tag{2}$$

$$T_r = T/T_C \tag{3}$$

where P and P_C are the pressure and critical pressure in megapascals, respectively; P_r is the reduced pressure; T and T_C are the temperature and critical temperature in kelvins, respectively; and T_r is the reduced temperature. a, b, c, and d are the Wagner parameters, and they are tabulated in Table 4. The correlation was conducted by treating all data points equally.

Table 6. Critical Parameters of the DME (1) + Butane (2) System

x_1[a]	T_C/K	P_C/MPa	ρ_C/kg m^{-3}	x_1[b] (optical cell base deviation/%)[c]	x_1[d] (optical cell base deviation/%)[e]
0.0000	425.16	3.787	225	0.0000 (0.00)	0.0000 (0.00)
0.2332	416.82	4.162	235	0.2323 (0.39)	0.2312 (0.86)
0.3943	411.47	4.392	242	0.3955 (−0.30)	0.3951 (−0.20)
0.5529	406.81	4.597	245	0.5519 (0.18)	0.5541 (−0.22)
0.7405	402.38	4.843	258	0.7467 (−0.84)	0.7419 (−0.19)
0.8958	400.17	5.074	265	0.8910 (0.54)	0.8954 (0.05)
1.0000	399.63	5.267	271	1.0000 (0.00)	1.0000 (0.00)
			AAD:	**(0.32)**	**(0.21)**

[a] Mole fraction in the optical cell. [b] Mole fraction calculated from the weight ratio. [c] $100(x_{\text{optical cell}} - x_{\text{feed}})/x_{\text{optical cell}}$. [d] Mole fraction in the null-pressure detector and variable volume vessels. [e] $100(x_{\text{optical cell}} - x_{\text{null-pressure detector}})/x_{\text{optical cell}}$.

Table 7. Critical Parameters of the DME (1) + 2-Methyl Propane (2) System

x_1[a]	T_C/K	P_C/MPa	ρ_C/kg m^{-3}	x_1[b] (optical cell base deviation/%)[c]	x_1[d] (optical cell base deviation/%)[e]
0.0000	407.81	3.633	225	0.0000 (0.00)	0.0000 (0.00)
0.2152	403.03	3.955	235	0.2175 (−1.07)	0.2141 (0.51)
0.4006	399.87	4.218	238	0.4019 (−0.32)	0.4000 (0.15)
0.5990	397.66	4.503	246	0.5974 (0.27)	0.5968 (0.37)
0.7493	397.23	4.746	256	0.7478 (0.20)	0.7492 (0.01)
0.8907	398.01	5.013	265	0.8874 (0.37)	0.8904 (0.03)
1.0000	399.63	5.267	271	1.0000 (0.00)	1.0000 (0.00)
			AAD:	**(0.32)**	**(0.15)**

[a] Mole fraction in the optical cell. [b] Mole fraction calculated from the weight ratio. [c] $100(x_{\text{optical cell}} - x_{\text{feed}})/x_{\text{optical cell}}$. [d] Mole fraction in the null-pressure detector and variable volume vessels. [e] $100(x_{\text{optical cell}} - x_{\text{null-pressure detector}})/x_{\text{optical cell}}$.

Critical Parameters of Mixtures. Figures 4 and 5 and Tables 5−7 show the critical parameters of the binary mixtures of DME and hydrocarbons. As previously reported, the critical density data showed a wider spread compared with critical temperature and pressure. From the tables, it is clear that, as described in the Experimental Section, there are compositional differences between the samples recovered from the optical cell and null-pressure detector. The larger the boiling point and critical temperature difference, the larger the average absolute deviation (AAD) of the composition. This fact suggests the existence of a small temperature difference between the optical cell and null-pressure detector that results in composition fluctuations even with the extreme care taken to reduce the temperature fluctuation. However, as the AADs are smaller than 1% for all three systems and considering the composition dependence of the critical properties given in Figure 4, there will be small effects on the critical parameters measured in this study. The tendency that the larger the difference in normal boiling point, the greater the AAD of the composition difference is similar to that observed in previous reports.[9,10] Some researchers have developed variable volume type[15] and expansion type[16] apparatus for critical parameter measurements and used them to measure pure fluids[17] and fluid mixtures.[18−20] For pure substances, no problems should arise in the experimental procedures and results. However, in the case of the mixtures, none of the reports mention their detailed compositions. As described in the Experimental Section, keeping the mixture under the supercritical condition for several hours was not sufficient to achieve compositional equilibration. From the composition fluctuation observed in previous and present studies, where extensive care for the composition equilibration was taken, it is clear that the composition analysis must be included in these kind of measurements.

In the figures, the estimated critical points of the DME + butane system reported by Defemandez et al.[21] are also plotted for comparison (open rectangles). These authors reported that the system has an azeotropic point at the low DME concentration. Figure 5 suggests that the DME + 2-methyl propane system might also have an azeotropic point.

Table 8. Correlated Results

system	parameters	AAD/%
DME + propane	$\Delta_T = -6.686$	T_C: 0.14
	$\Delta_P = 0.031\,89$	P_C: 0.25
	$\Delta_V = -10.44$	ρ_C: 0.54
DME + butane	$\Delta_T = -19.47$	T_C: 0.21
	$\Delta_P = 0.5952$	P_C: 0.98
	$\Delta_V = 40.87$	ρ_C: 1.00
DME + 2-methyl propane	$\Delta_T = -13.80$	T_C: 0.18
	$\Delta_P = 0.4614$	P_C: 0.70
	$\Delta_V = -36.78$	ρ_C: 0.78

For the correlation of the critical loci of binary HFC mixtures, Higashi proposed the following equations:[22,23]

$$T_{\mathrm{Cm}} = \theta_1 T_{\mathrm{C1}} + \theta_2 T_{\mathrm{C2}} + 2\theta_1\theta_2\Delta_T \tag{4}$$

$$V_{\mathrm{Cm}} = \theta_1 V_{\mathrm{C1}} + \theta_2 V_{\mathrm{C2}} + 2\theta_1\theta_2\Delta_V \tag{5}$$

$$P_{\mathrm{Cm}} = \theta_1 P_{\mathrm{C1}} + \theta_2 P_{\mathrm{C2}} + 2\theta_1\theta_2\Delta_P \tag{6}$$

$$\rho_{\mathrm{Cm}} = M_{\mathrm{m}}/V_{\mathrm{Cm}} \tag{7}$$

$$M_{\mathrm{m}} = x_1 M_1 + (1 - x_1)M_2 \tag{8}$$

$$\theta_i = \frac{x_i {V_{\mathrm{C}i}}^{2/3}}{\sum_{j=1}^{2} x_j {V_{\mathrm{C}j}}^{2/3}}, \quad i = 1, 2 \tag{9}$$

where $T_{\mathrm{C}i}$, $V_{\mathrm{C}i}$, and $P_{\mathrm{C}i}$ are the critical temperature, critical molar volume, and critical pressure of component i, respectively; x is the mole fraction; M_i is the molecular weight of component i; ϑ_i is the surface fraction of component i defined by eq 9 in terms of the composition and critical molar volumes of the pure components; and Δ_T, Δ_V, and Δ_P are the fitting parameters for critical temperature, volume, and pressure, respectively, determined from the experimental results obtained in this study. The subscript "m" signifies mixture. The experimental data obtained in this study are correlated with the equations.

The correlated results are shown as lines in Figures 4 and 5 and are summarized in Table 8. As shown in the figures and table, the AADs of the critical parameters are $< \pm 1\%$. However, as mentioned above, the AADs of the critical density are much greater than those of the critical temperature.

4. Conclusion

We have measured the critical parameters of three binary systems of DME with propane, butane, and 2-methyl propane, respectively, with uncertainties of ±10 mK in temperature, ±0.5 kPa in pressure, ±1 kg m^{-3} in density, and ±0.5% in composition. The experimental data spread of the critical density was larger than that of the critical temperature and pressure, presumably due to the difficulty in measuring the density near the critical condition where it changes sharply with only minor changes in temperature and pressure. The experimental results were correlated with equations proposed by Higashi. The maximum AAD was <1% for all critical parameters.

Literature Cited

(1) Sorenson, S. C. Dimethyl ether in diesel engines: Progress and perspectives. *J. Eng. Gas Turbines Power* **2001**, *123*, 652−658.

(2) Dahlhoff, G.; Pfennig, A. Vapor−Liquid Equilibria in Quaternary Mixtures of Dimethyl Ether + *n*-Butane + Ethanol + Water. *J. Chem. Eng. Data* **2000**, *45*, 887−892.

(3) Elbaccouch, M. M.; Elliott, J. R. High-Pressure Vapor−Liquid Equilibrium for Dimethyl Ether + Ethanol and Dimethyl Ether + Ethanol + Water. *J. Chem. Eng. Data* **2000**, *45*, 1080−1087.

(4) Daiguji, H.; Hihara, E., Vapor−Liquid Equilibrium for Dimethyl Ether + Propyl Acetate. *J. Chem. Eng. Data* **2003**, *48*, 266−271.

(5) Florusse, L. J.; Fornari, T.; Bottini, S. B.; Peters, C. J. Phase behavior of the binary system near-critical dimethylether and tripalmitin: measurements and thermodynamic modeling. *J. Supercrit. Fluids* **2002**, *22*, 1−13.

(6) Mench, M. M.; Chance, H. M.; Wang, C. Y. Direct dimethyl ether polymer electrolyte fuel cells for portable applications. *J. Electrochem. Soc.* **2004**, *151*, A144−A150.

(7) Yasumoto, M.; Yamada, Y.; Murata, J.; Urata, S.; Otake, K. Critical Parameters and Vapor Pressure Measurements of Hydrofluoroethers at High Temperatures. *J. Chem. Eng. Data* **2003**, *48*, 1368−1379.

(8) Otake, K.; Yasumoto, M.; Yamada, Y.; Murata, J.; Urata, S. Critical Parameters and Vapor Pressure Measurements of Potential Replacements for Chlorofluorocarbonss: Four Hydrofluoroketones and a Hydrofluoroamine. *J. Chem. Eng. Data* **2003**, *48*, 1380−1383.

(9) Otake, K.; Uchida, Y.; Yasumoto, M.; Yamada, Y.; Furuya, T.; Ochi, K. Critical Properties of Four HFE + HFC Binary Systems: Trifluoromethoxymethane (HFE-143m) + Pentafluoroethane (HFC-125), + 1,1,1,2-Tetrafluoroethane (HFC-134a), + 1,1,1,2,3,3,3-Heptafluoropropane (HFC-227ea), and + 1,1,1,2,3,3-Hexafluoropropane (HFC-236ea). *J. Chem. Eng. Data* **2004**, *49*, 1615−1621.

(10) Uchida, Y.; Yasumoto, M.; Yamada, Y.; Ochi, K.; Furuya, T.; Otake, K. Critical Properties of Four HFE + HFC Binary Systems: Trifluoromethoxymethane (HFE-143m) + Pentafluoroethane (HFC-125), + 1,1,1,2-Tetrafluoroethane (HFC-134a), + 1,1,1,2,3,3,3-Heptafluoropropane (HFC-227ea), and + 1,1,1,2,3,3-Hexafluoropropane (HFC-236ea). *J. Chem. Eng. Data* **2004**, *49*, 1643−1647.

(11) Poling, B. E.; Prausnitz, J. M.; O'Connell, J. P. *The Properties of Gases and Liquids*, 5th ed.; McGraw-Hill: New York, 2000.

(12) Ambrose, D.; Tsonopoulos, C. Vapor−Liquid Critical Properties of Elements and Compounds. 2. Normal Alkanes. *J. Chem. Eng. Data* **1995**, *40*, 531−546.

(13) Daubert, T. E. Vapor−Liquid Critical Properties of Elements and Compounds. 5. Branched Alkanes and Cycloalkanes. *J. Chem. Eng. Data* **1996**, *41*, 365−372.

(14) Kudchadker, A. P.; Ambrose, D.; Tsonopoulos, C. Vapor−Liquid Critical Properties of Elements and Compounds. 7. Oxygen Compounds Other than Alkanols and Cycloalkanols. *J. Chem. Eng. Data* **2001**, *46*, 457−479.

(15) Suehiro, Y.; Nakajikma, M.; Yamada, K.; Uemtsu, M. Critical parameters of {xCO2+(1-x)CHF3} for x=(1.0000, 0.7496, 0.5013, and 0.2522). *J. Chem. Thermodyn.* **1996**, *28*, 1153−1164.

(16) Okazaki, S.; Higashi, Y.; Takaishi, Y.; Uematsu, M.; Watanabe, K. Procedures for determining the critical parameters of fluids. *Rev. Sci. Instrum.* **1983**, *54*, 21−25.

(17) Higashi, Y. Experimental determination of the critical locus for the difluoromethane (R32) and propane (R290) system. *Fluid Phase Equilib.* **2004**, *219*, 99−103.

(18) Kayukawa, Y.; Watanabe, K. PTx Measurements for Gas-Phase Pentafluoroethane + Propane Mixtures by the Burnett Method. *J. Chem. Eng. Data* **2001**, *46*, 1025−1030.

(19) Kayukawa, Y.; Tada, S.; Zhang, H.-L.; Watanabe, K. Measurements of Gas-Phase PVTx Properties for the Ternary Mixtures Difluoromethane (1) + Pentafluoroethane (2) + 1,1,1-Trifluoroethane (3). *J. Chem. Eng. Data* **2002**, *47*, 1406−1410.

(20) Naganuma, S.; Mizote, A.; Watanabe, K. Measurements of PVTx and Saturation Properties for the Binary 1,1,1,2-Tetrafluoroethane + Propane System. *J. Chem. Eng. Data* **2001**, *46*, 1031−1034.

(21) Defernandez, M. E. P.; Calado, J. C. G.; Zollweg, J. A.; Streett, W. B. Vapor-Liquid-Equilibria In The Binary-System Dimethyl Ether Plus N-Butane From 282.9 To 414.5-K At Pressures To 4.82 MPa. *Fluid Phase Equilib.* **1992**, *74*, 289−302.

(22) Higashi, Y. Vapor-Liquid Equilibrium of Ternary Mixtures of the Refrigerants R32, R125, and R134a. *Int. J. Refrig.* **1995**, *18*, 534−543.

(23) Higashi, Y. Vapor Liquid Critical Surface of Ternary Difluoromethane + Pentafluoroethane + 1,1,1,2-Tetrafluoroethane (R-32/125/134a) Mixtures. *Int. J. Thermophys.* **1999**, *20*, 1483−1459.

(24) Noles, J. R. *Vapor-Liquid Equilibria of Solvating Binary Mixtures*; Cornell University: New York, 1991.

(25) Noles, J. R.; Zollweg, J. A. Isothermal Vapor-Liquid-Equilibrium For Dimethyl Ether + Sulfur-Dioxide. *Fluid Phase Equilib.* **1991**, *66*, 275−289.

(26) Noles, J. R.; Zollweg, J. A. Vapor−Liquid Equilibrium for Chlorodifluoromethane plus Dimethyl Ether from 283 to 395 K at Pressures to 5.0 MPa. *J. Chem. Eng. Data* **1992**, *37*, 306−310.

(27) Wu, J.; Liu, Z.; Pan, J.; Zhao, X. Vapor Pressure Measurements of Dimethyl Ether from (233 to 399) K. *J. Chem. Eng. Data* **2004**, *49*, 32−34.
(28) Wu, J. T.; Liu, Z. G.; Wang, B.; Pan, J. Measurement of the Critical Parameters and the Saturation Densities of Dimethyl Ether. *J. Chem. Eng. Data* **2004**, *49*, 704−708.
(29) Tomoya, T. Saturation pressure and PVT relationship of DME and DME mixtures with ethane, propane, butane, water, and ethylene glycol. Manuscript in preparation.
(30) Stryjek, R.; Vera, J. H. PRSV: An Improved Peng−Robinson Equation of State for Pure Compounds and Mixtures. *J. Chem. Eng. Data* **1986**, *31*, 323−333.
(31) Higashi, Y. Determination of the Critical Parameters for Propane (R290) and Isobutane(R600a). *Proc. Jpn. Symp. Thermophys. Prop., 23rd* **2002**, 175−177.
(32) Sengers, J. M. H. L.; Kamgar-Parsi, B.; Sengers, J. V. Thermodynamic Properties of Isobutane in the Critical Region. *J. Chem. Eng. Data* **1983**, *28*, 354−362.

Received for review September 21, 2004. Accepted December 14, 2004.

JE0496589